On the liquid drop model mass formulas and α decay of the heaviest nuclei

G. Royer, M. Guilbaud, A. Onillon and H.F. Zhang[*]
Subatech Laboratory, Nantes, France

Abstract
The coefficients of different macro-microscopic Liquid Drop Model mass formulas have been determined by a least square fitting procedure to 2027 experimental atomic masses. A rms deviation of 0.54 MeV can be reached. The remaining differences come mainly from the determination of the shell and pairing energies. Extrapolations are compared to 161 new experimental masses and to 656 mass evaluations. The different fits lead to a surface energy coefficient of around 17-18 MeV. Finally, α decay potential barriers are revisited and predictions of α decay half-lives of still unknown superheavy elements are given from previously proposed analytical formulas and from extrapolated Q_α values.

1 Introduction

Predictions of the masses of exotic nuclei close to the proton and neutron drip lines and in the superheavy element region must still be improved. Beyond the Bethe-Weizsäcker formula [1, 2] and beside the statistical Thomas-Fermi model [3] and the microscopic Hartree-Fock self-consistent mean field approaches [4], different versions of the macro-microscopic Liquid Drop Model mass formula and nuclear radii have been investigated [5]. The α decay potential barriers deciding the half-lives of the heaviest elements have been precised and half-lives of still unknown superheavy nuclei have been provided.

2 Macro-microscopic Liquid Drop Model binding energy

Different subsets of the following expansion of the nuclear binding energy have been considered :

$$B = a_v\left(1-k_vI^2\right)A - a_s\left(1-k_sI^2\right)A^{\frac{2}{3}} - a_k\left(1-k_kI^2\right)A^{\frac{1}{3}} - \frac{3}{5}\frac{e^2Z^2}{R_0} + f_p\frac{Z^2}{A} + a_{c,exc}\frac{Z^{\frac{4}{3}}}{A^{\frac{1}{3}}} - E_{pair} - E_{shell} - E_{Wigner}. \quad (1)$$

The first term gives the volume energy corresponding to the saturated exchange force and infinite nuclear matter. I^2A is the asymmetry energy of the Bethe-Weizsäcker mass formula. The second term is the surface energy. It takes into account the deficit of binding energy of the nucleons at the nuclear surface and corresponds to semi-infinite nuclear matter. The third term is the curvature energy. It is a correction to the surface energy resulting from local properties and consequently depending on the mean local curvature. This term is considered in the TF model [3] but not in the FRLDM [6]. The fourth term gives the decrease of binding energy due to the repulsion between the protons. Different formulas will be assumed for the charge radius. The Z^2/A term is the diffuseness correction to the basic sharp radius Coulomb energy term (called also the proton form-factor correction to the Coulomb energy in [6]). The $Z^{4/3}/A^{1/3}$ term is the charge exchange correction term. The pairing and shell energies of the recent Thomas-Fermi model [3, 5] have been used and four versions of the Wigner term have been taken into account, namely: $W_1 = |I|$, $W_2 = |N-Z| \times e^{-(A/50)^2}$, $W_3 = |N-Z| \times e^{-A/35}$ and $W_4 = e^{-80I^2}$. To obtain the coefficients of the selected expansions by a least square fitting procedure, the masses of

[*]On leave from School of Nuclear Science and Technology, Lanzhou University, People's Republic of China

the 2027 nuclei verifying the two conditions : N and Z higher than 7 and the one standard deviation uncertainty on the mass lower than 150 keV [7] have been used.

In Table 1 the Coulomb energy is calculated assuming $R_0 = 1.28A^{1/3} - 0.76 + 0.8A^{-1/3}$, expression previously used in fusion, fission and alpha decay studies [8, 9]. This formula proposed in Ref. [10] simulates rather a central radius. The diffuseness correction term or the charge exchange correction term plays the main role to improve the accuracy of the mass formulas. The W_2 and W_3 terms are as efficient as the usual W_1 term. The main advantage of the W_2 term is its relative continuity during the transition from one body to two body shapes. A rms deviation of 0.56 MeV can be reached. In Table 2 the charge radius is simply $R_0 = 1.16A^{1/3}$ fm. This often retained mean value does not allow to reach an accuracy better than 0.72 MeV.

Table 1: Coefficient values and root mean square mass deviation (in MeV). The theoretical shell and pairing energies are taken into account. The Coulomb energy is determined by $0.6e^2Z^2/(1.28A^{1/3} - 0.76 + 0.8A^{-1/3})$.

a_v	k_v	a_s	k_s	f_p	$a_{c,exc}$	W_1	W_2	W_3	W_4	σ
15.8548	1.7281	17.3228	0.8179	-	-	-	-	-	-	1.402
15.8427	1.7368	17.2607	0.8727	-	-	-	0.4083	-	-	1.368
15.8276	1.7681	17.176	1.0540	-	-	-	-	1.1872	-	1.334
15.8328	1.8931	17.1077	1.9361	-	-	41.003	-	-	-	1.199
16.038	1.9801	18.4563	2.2201	-	-	-	-	-	-8.4670	0.994
15.5172	1.7753	17.9474	1.6575	2.1401	-	-	-	-	-	0.692
15.2508	1.7840	17.9475	1.6577	-	2.0195	-	-	-	-	0.691
15.6233	1.8412	18.1709	1.92097	1.7987	-	-	-	-	-2.4136	0.661
15.3989	1.8492	18.1703	2.0320	-	1.6983	-	-	-	-2.4059	0.661
15.5002	1.7860	17.8829	1.7290	2.1612	-	-	0.4645	-	-	0.597
15.2312	1.7949	17.8831	1.7291	-	2.0393	-	0.4641	-	-	0.596
15.5003	1.8088	17.8136	1.8401	2.1032	-	-	-	0.9951	-	0.591
15.5389	1.8585	17.7736	2.1451	1.9299	-	21.437	-	-	-	0.591
15.2986	1.8690	17.7739	2.1444	-	1.8212	21.401	-	-	-	0.590
15.5899	1.8840	17.9004	2.2326	1.7779	-	19.554	-	-	-1.2050	0.583
15.3684	1.8924	17.9003	2.2316	-	1.6783	19.528	-	-	-1.2004	0.582
15.5868	1.8602	18.0012	2.0434	1.8294	-	-	-	0.9428	-1.9495	0.567
15.3587	1.8687	18.0007	2.0427	-	1.7272	-	-	0.9424	-1.9425	0.567
15.6096	1.8543	18.1132	2.0021	1.80856	-	-	0.4700	-	-2.4953	0.558
15.3841	1.8625	18.1127	2.0014	-	1.7073	-	0.4696	-	-2.4886	0.558

In the formulas (2)-(6) the reduced radius r_0 is provided by the adjustment to the experimental masses. The rms deviations are respectively : 0.633, 0.579, 0.610, 0.564 and 0.543 MeV. The Wigner terms are more efficient than the curvature term but they induce a high value of r_0. The combination of two Wigner terms allows to reach a very good accuracy. The radius $R_0 = 1.2257\ A^{1/3}$ fm is imposed in the formula (7). It has been obtained by an adjustment on 782 ground state charge radii [11]. It allows also to obtain a good accuracy of 0.584 MeV contrarily to the value $r_0 = 1.16$ fm. In the last formula (8) the radius is taken as the central radius previously used in Table 1 and $\sigma = 0.558$ MeV. So it it possible to obtain accurate mass formulas with a large constant reduced radius r_0 or with a more sophisticated central radius corresponding to a smaller value of r_0 increasing with the mass.

$$B = 15.4122\left(1 - 1.7116I^2\right)A - 17.5371\left(1 - 1.4015I^2\right)A^{\frac{2}{3}} - 0.6\frac{e^2Z^2}{1.2177A^{\frac{1}{3}}} + 1.3736\frac{Z^2}{A} - E_{pair} - E_{shell}. \quad (2)$$

Table 2: Coefficient values (in MeV) and root mean square deviation. The theoretical shell and pairing energies are taken into account. The Coulomb energy is determined by $0.6e^2Z^2/(1.16A^{1/3})$.

a_v	k_v	a_s	k_s	f_p	$a_{c,exc}$	W_1	W_2	W_3	W_4	σ
16.0975	1.6145	18.4883	0.3684	-	-	-	-	-	-	1.757
16.1273	1.5934	18.642	0.2466	-	-	-	-1.0105	-	-	1.583
16.1388	1.5552	18.711	0.0449	-	-	-	-	-1.8053	-	1.631
16.1017	1.5836	18.5293	0.1728	-	-	-7.8076	-	-	-	1.751
16.3374	1.9404	19.9732	2.0989	-	-	-	-	-	-11.0907	1.186
15.7511	1.6597	19.1291	1.1916	2.1955	-	-	-	-	-	1.233
15.4781	1.6665	19.129	1.1914	-	2.0710	-	-	-	-	1.233
16.0616	1.8498	19.7833	1.9150	1.1963	-	-	-	-	-7.0645	1.079
15.9131	1.8552	19.7832	1.9149	-	1.1278	-	-	-	-7.0659	1.079
15.7862	1.6384	19.2616	1.0584	2.1520	-	-	-0.9546	-	-	1.001
15.5185	1.6457	19.2616	1.0583	-	2.0302	-	-0.9550	-	-	1.001
15.7855	1.5936	19.3991	0.8600	2.2700	-	-	-	-2.0089	-	0.996
15.7174	1.5313	19.3998	0.5023	2.5229	-	-33.3855	-	-	-	1.098
15.4034	1.5363	19.4002	0.5014	-	2.3807	-33.4319	-	-	-	1.098
16.1454	1.7460	20.4634	1.2294	1.2486	-	-49.1756	-	-	-10.1039	0.739
15.9900	1.7505	20.4634	1.2289	-	1.1782	-49.1935	-	-	-10.1026	0.739
16.1478	1.8064	20.1843	1.6570	1.1238	-	-	-	-2.2277	-8.161	0.722
16.0082	1.8058	20.1842	1.6568	-	1.0597	-	-	-2.2280	-8.1614	0.722
16.0889	1.8245	19.8986	1.7673	1.1767	-	-	-0.9394	-	-6.9010	0.814
15.9426	1.8295	19.8984	1.7670	-	1.1098	-	-0.9397	-	-6.9003	0.814

$$B = 15.3529\left(1-1.8084I^2\right)A - 16.9834\left(1-1.9647I^2\right)A^{\frac{2}{3}} - 0.6\frac{e^2Z^2}{1.2324A^{\frac{1}{3}}} + 0.9675\frac{Z^2}{A} - 21.3975|I| - E_{pair} - E_{shell}. \quad (3)$$

$$B = 15.4529\left(1-1.8722I^2\right)A - 18.0588\left(1-2.7716I^2\right)A^{\frac{2}{3}} - 0.6\frac{e^2Z^2}{1.2204A^{\frac{1}{3}}} + 1.3712\frac{Z^2}{A} + 1.348\left(1-45.I^2\right)A^{\frac{1}{3}} - E_{pair} - E_{shell}. \quad (4)$$

$$B = 15.2508\left(1-1.7489I^2\right)A - 16.8015\left(1-1.6077I^2\right)A^{\frac{2}{3}} - 0.6\frac{e^2Z^2}{1.2426A^{\frac{1}{3}}} + 1.0736\frac{Z^2}{A} - 0.6806|N-Z| \times e^{-(A/50)^2} - E_{pair} - E_{shell}. \quad (5)$$

$$B = 15.4133\left(1-1.7962I^2\right)A - 17.3079\left(1-1.7858I^2\right)A^{\frac{2}{3}} - 0.6\frac{e^2Z^2}{1.2318A^{\frac{1}{3}}} + 0.8956\frac{Z^2}{A} - 0.4838|N-Z| \times e^{-(A/50)^2} + 2.2 \times e^{-80I^2} - E_{pair} - E_{shell}. \quad (6)$$

$$B = 15.3848\left(1-1.7837I^2\right)A - 17.1947\left(1-1.8204I^2\right)A^{\frac{2}{3}} - 0.6\frac{e^2Z^2}{1.2257A^{\frac{1}{3}}} + 1.1035\frac{Z^2}{A} - 16.606|I| - E_{pair} - E_{shell}. \quad (7)$$

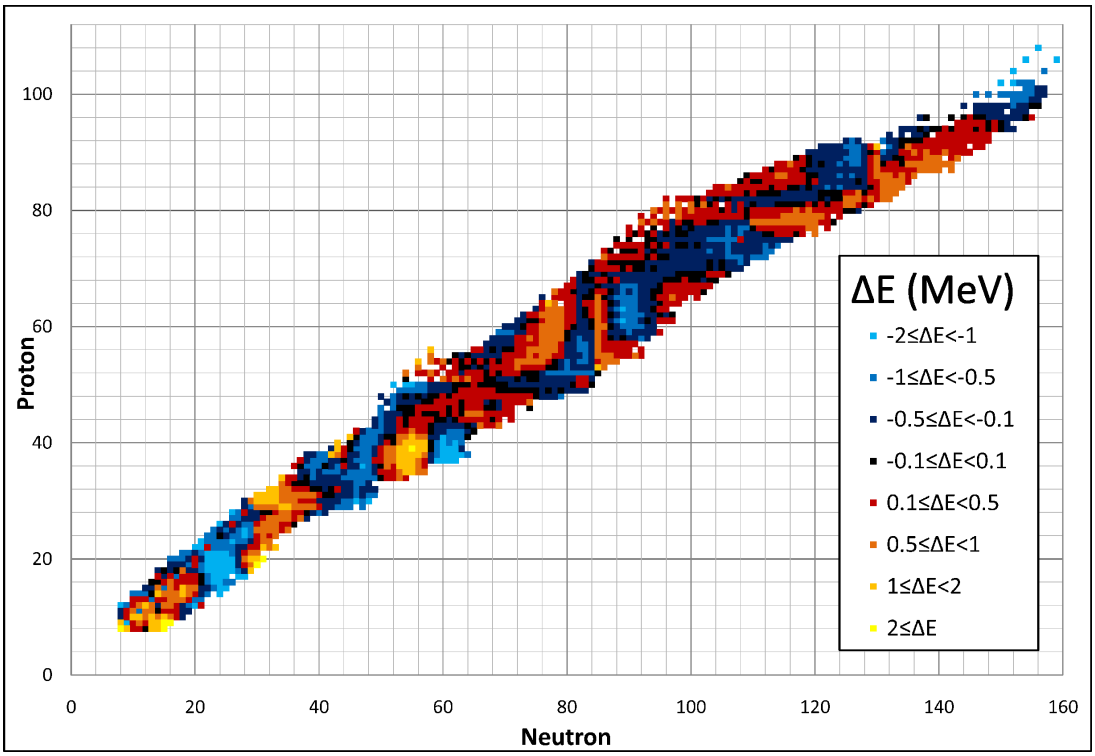

Fig. 1: Difference between the theoretical masses obtained with the formula (8) and the experimental masses of the 2027 selected nuclei.

$$B = 15.6096\left(1-1.8543I^2\right)A - 18.1132\left(1-2.0021I^2\right)A^{\frac{2}{3}} - 0.6\frac{e^2Z^2}{1.28A^{\frac{1}{3}} - 0.76 + 0.8A^{-\frac{1}{3}}}$$
$$+1.8086\frac{Z^2}{A} - 0.47|N-Z| \times e^{-(A/50)^2} + 2.4954 \times e^{-80I^2} - E_{pair} - E_{shell}. \quad (8)$$

The difference between the theoretical masses obtained with the formula (8) and the experimental masses of the 2027 nuclei used for the adjustment of the coefficients is indicated in Figure 1. The more the colour is dark the more the accuracy is high. The distribution of the nuclei in each error range is given explicitly in Figure 2. The errors are slightly larger for the light nuclei. The same behaviour is encountered by all the mass models. Nevertheless the error is very rarely higher than 2 MeV.

3 Extrapolation to new nuclear masses

Since the last mass evaluation [7] other masses have been newly or more precisely obtained. The predictions given by the formula (8) (not readjusted) for 161 new masses are compared with the experimental data in Figure 3. The accuracy is correct in the whole mass range showing the predictability of such formulas. Finally, the predictions for 656 other nuclei for which the mass is still unknown are compared to the extrapolations given in Ref. [7]. The explicit values will be given in a forthcoming paper. Without readjustment the formula (8) leads to $\sigma = 0.73$ MeV for the 2844 nuclei. It must be noticed that the errors in the extrapolations are not known and may be large.

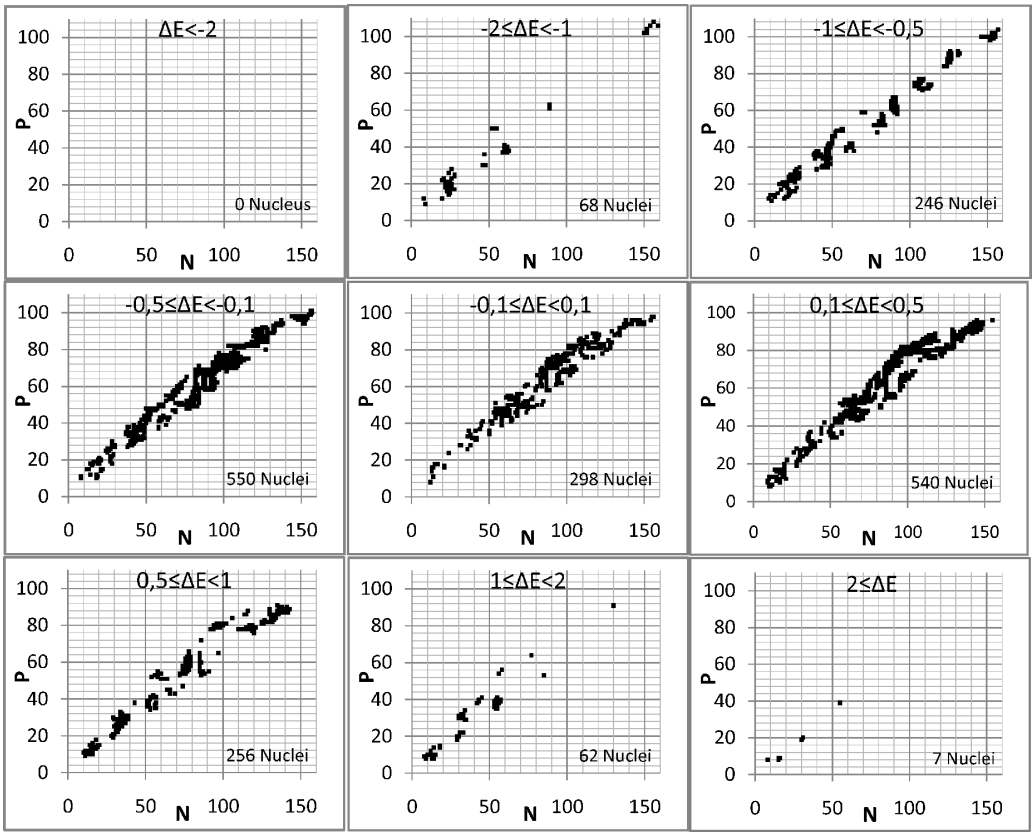

Fig. 2: Distribution of the 2027 nuclei in each error range.

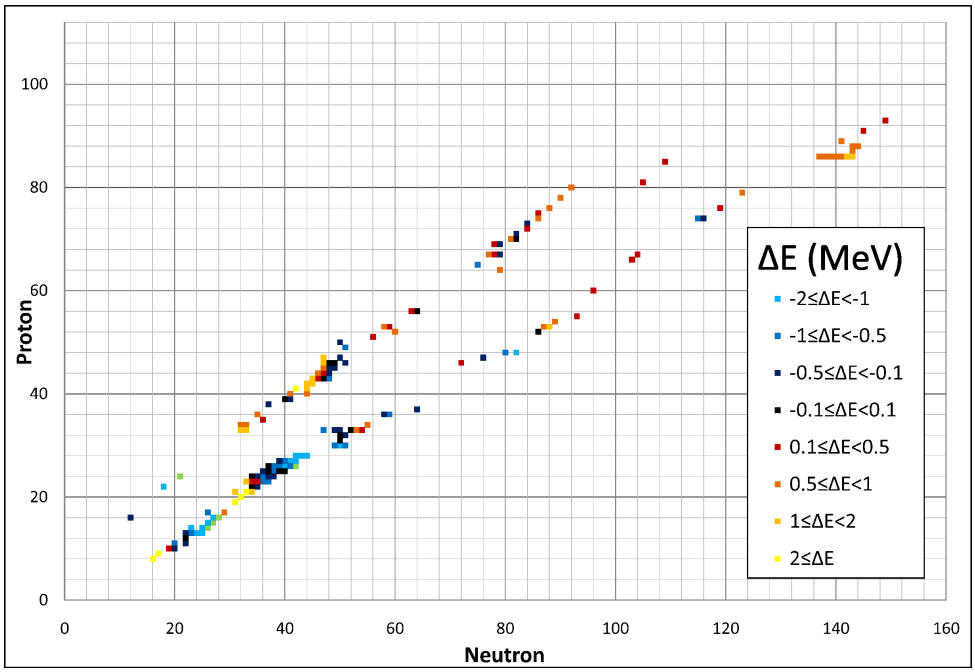

Fig. 3: Difference between the theoretical masses obtained with the formula (8) and 161 new experimental masses.

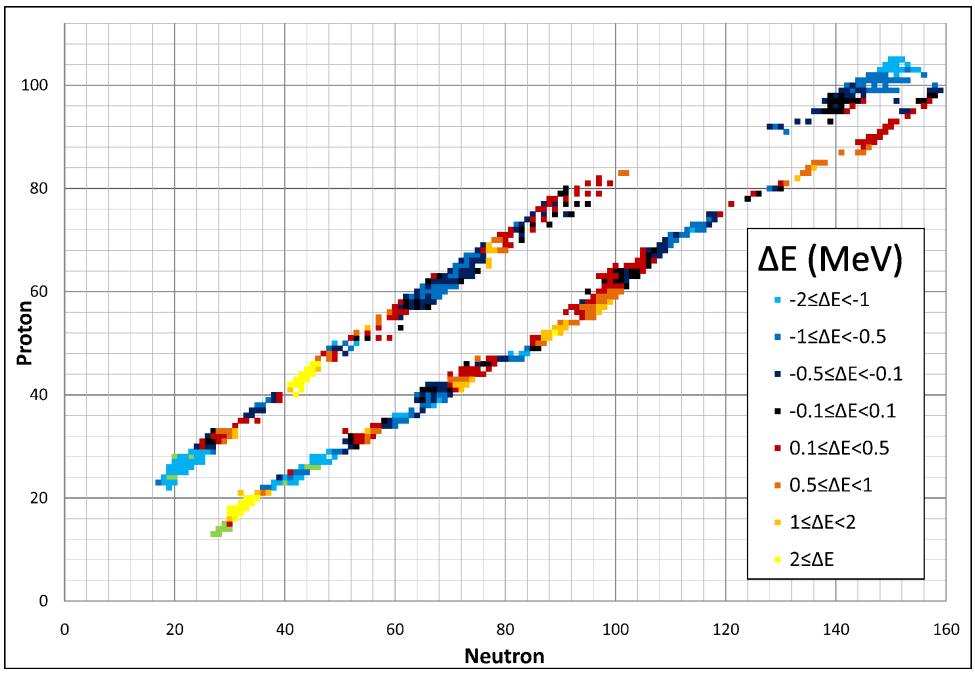

Fig. 4: Difference between the theoretical masses obtained with the formula (8) and 656 extrapolated masses.

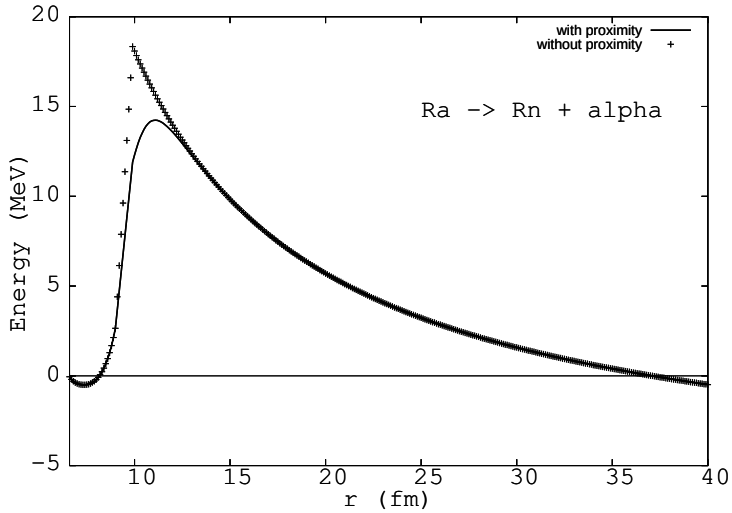

Fig. 5: Alpha decay barriers of ^{222}Ra.

4 α decay potential barrier

Often, the potential barrier standing against α decay is taken as the pure Coulomb barrier since the integration of the Schrödinger equation is easier. Such a barrier is unrealistic since it cannot reproduce the fusion barrier characteristics. It is necessary to take into account the proximity forces between the nucleons in regard in the neck or gap between the two nuclei. The alpha decay barrier of ^{222}Ra is displayed in Figure (5). The proximity energy lowers the barrier height by around 5 MeV and moves the barrier top to a more external position corresponding to two separated spheres maintained in unstable equilibrium by the balance between the repulsive Coulomb forces and the attractive nuclear proximity forces. The Q value has been introduced empirically in adding at the macroscopic energy of the mother nucleus the difference between the experimental and theoretical Q value with a linear attenuation factor vanishing at the contact point between the nascent fragments [9].

The following formula gives accurately the distance between the mass centers at the α barrier top. A and Z are the mass and charge of the mother nucleus.

$$R = 2.536 + 1.1157\ [4^{\frac{1}{3}} + (A-4)^{\frac{1}{3}}]\ \ fm. \tag{9}$$

The height of the barrier against α decay can be determined using:

$$E = -1.43 + \frac{e^2 \times 2 \times (Z-2)}{2.536 + 1.1157[4^{\frac{1}{3}} + (A-4)^{\frac{1}{3}}]} - Q\ \ MeV. \tag{10}$$

A fitting procedure led to the following formulas to calculate the α decay half-lives respectively for the even(Z)-even(N), even-odd, odd-even and odd-odd nuclei. The rms deviation are respectively 0.285, 0.39, 0.36 and 0.35.

$$log_{10}\left[T_{1/2}(s)\right] = -25.31 - 1.1629A^{1/6}\sqrt{Z} + \frac{1.5864Z}{\sqrt{Q_\alpha}}, \tag{11}$$

$$log_{10}\left[T_{1/2}(s)\right] = -26.65 - 1.0859A^{1/6}\sqrt{Z} + \frac{1.5848Z}{\sqrt{Q_\alpha}}, \tag{12}$$

$$log_{10}\left[T_{1/2}(s)\right] = -25.68 - 1.1423A^{1/6}\sqrt{Z} + \frac{1.592Z}{\sqrt{Q_\alpha}}, \tag{13}$$

$$log_{10}\left[T_{1/2}(s)\right] = -29.48 - 1.113A^{1/6}\sqrt{Z} + \frac{1.6971Z}{\sqrt{Q_\alpha}}. \tag{14}$$

5 α decay half-live of unknown superheavy elements

The predictions within these formulas have been compared [12] with new experimental data ranging from ^{105}Te to the superheavy elements and other theoretical predictions. The agreement is quite correct. The fact that the partial α decay half-lives of the superheavy elements follow these simple formulas seems to prove that the experimental data are consistent with the formation of a cold and relatively compact composite nuclear system. Thus predictions of the partial α decay half-lives of other still unknown superheavy nuclei seem reliable and are displayed in Table 3. The assumed Q_α values are taken from the atomic mass evaluation table [7]. For several nuclei the half-live reaches some minutes and even some hours. The possibility to form such nuclei remains completely questionable.

6 Conclusion

The coefficients of different macro-microscopic Liquid Drop Model mass formulas have been determined by an adjustment to 2027 experimental atomic masses. A rms deviation of 0.54 MeV can be reached. The remaining differences come mainly from the determination of the shell and pairing energies. A large constant coefficient $r_0 = 1.22 - 1.23$ fm or a small value increasing with the mass can be used. Extrapolations are compared to 161 new experimental masses and to 656 mass evaluations of exotic nuclei. The different fits lead always to a surface energy coefficient of around 17-18 MeV. α decay potential barriers are also revisited and predictions of α decay half-lives of still unknown superheavy elements are given from previously proposed analytical formulas and from extrapolated Q_α values.

References

[1] C.F. von Weizsäcker, *Z. Physik* **96** (1935) 431.

[2] H.A. Bethe, R.F. Bacher, *Rev. Mod. Phys.* **8** (1936) 82.

[3] W.D. Myers, W.J. Swiatecki, *Nucl. Phys. A* **601** (1996) 141.

[4] M. Samyn, S. Goriely, P.-H. Heenen, J.M. Pearson, F. Tondeur, *Nucl. Phys. A* **700** (2002) 142.

Table 3: Predicted α-decay half-lives using the formulas (11-14). The Q_α values are taken from the extrapolated data of Ref. [7].

$^{A}_{Z}$	Q	$T_{1/2}^{form.}$	$^{A}_{Z}$	Q	$T_{1/2}^{form.}$	$^{A}_{Z}$	Q	$T_{1/2}^{form.}$	$^{A}_{Z}$	Q	$T_{1/2}^{form.}$
$^{293}_{118}$	12.30	187 μs	$^{292}_{117}$	11.60	6.47 ms	$^{291}_{117}$	11.90	0.32 ms	$^{291}_{115}$	10.00	4.8 s
$^{290}_{115}$	10.30	4.2 s	$^{289}_{116}$	11.70	1.05 ms	$^{289}_{115}$	10.60	113 ms	$^{287}_{113}$	9.34	99.4 s
$^{286}_{113}$	9.68	61.5 s	$^{285}_{114}$	11.00	12 ms	$^{285}_{113}$	10.02	1.0 s	$^{284}_{112}$	9.30	25.1 s
$^{283}_{111}$	8.96	5.5 min	$^{282}_{112}$	9.96	0.297 s	$^{282}_{111}$	9.38	99.8 s	$^{281}_{112}$	10.28	0.2 s
$^{281}_{111}$	9.64	2.72 s	$^{281}_{110}$	8.96	4.6 min	$^{280}_{112}$	10.62	25.4 ms	$^{280}_{111}$	9.98	1.43 s
$^{279}_{112}$	10.96	3.88 ms	$^{279}_{109}$	8.70	7.72 min	$^{278}_{112}$	11.38	0.083 ms	$^{278}_{111}$	10.72	12.5 ms
$^{278}_{110}$	10.00	51.8 ms	$^{278}_{109}$	9.10	143 s	$^{277}_{112}$	11.62	0.12 ms	$^{277}_{111}$	11.18	0.28 ms
$^{277}_{110}$	10.30	39 ms	$^{277}_{109}$	9.50	1.48 s	$^{277}_{108}$	8.40	65.25 min	$^{276}_{111}$	11.32	0.39 ms
$^{276}_{110}$	10.60	1.47 ms	$^{276}_{108}$	8.80	40.6 s	$^{275}_{111}$	11.55	42.3 μs	$^{275}_{110}$	11.10	0.43 ms
$^{274}_{111}$	11.60	88.1 μs	$^{274}_{110}$	11.40	19.5 μs	$^{274}_{109}$	10.50	9.84 ms	$^{274}_{108}$	9.50	0.3 s
$^{274}_{107}$	8.50	48.45 min	$^{273}_{111}$	11.20	0.29 ms	$^{273}_{110}$	11.37	0.11 ms	$^{273}_{109}$	10.82	0.5 ms
$^{273}_{108}$	9.90	101 ms	$^{273}_{107}$	8.90	21.1 s	$^{272}_{110}$	10.76	0.697 ms	$^{272}_{109}$	10.60	5.74 ms
$^{272}_{108}$	10.10	6.9 ms	$^{272}_{106}$	8.30	6.38 min	$^{271}_{110}$	10.87	1.79 ms	$^{271}_{109}$	10.14	29.9 ms
$^{271}_{108}$	9.90	109.7 ms	$^{271}_{107}$	9.50	0.338 s	$^{270}_{110}$	11.20	0.067 ms	$^{270}_{109}$	10.35	30 ms
$^{270}_{108}$	9.30	1.4 s	$^{270}_{107}$	9.30	6.25 s	$^{270}_{106}$	9.10	0.99 s	$^{270}_{105}$	8.20	94.58 min
$^{269}_{109}$	10.53	3.12 ms	$^{269}_{108}$	9.63	0.68 s	$^{269}_{107}$	8.84	39 s	$^{269}_{106}$	8.80	37.5 s
$^{269}_{105}$	8.40	3.01 min	$^{268}_{110}$	11.92	1.84 μs	$^{268}_{109}$	10.73	3.07 ms	$^{268}_{108}$	9.90	28.6 ms
$^{268}_{107}$	9.08	35.4 s	$^{268}_{106}$	8.40	3.4 min	$^{268}_{105}$	8.20	102.7 min	$^{268}_{104}$	8.10	5.88 min
$^{267}_{110}$	12.28	1.57 μs	$^{267}_{109}$	10.87	0.49 ms	$^{267}_{108}$	10.12	32.9 ms	$^{267}_{107}$	9.37	0.97 s
$^{267}_{106}$	8.64	2.25 min	$^{267}_{105}$	7.90	205 min	$^{267}_{104}$	7.80	306 min	$^{266}_{109}$	10.996	0.69 ms
$^{266}_{108}$	10.336	2.16 ms	$^{266}_{107}$	9.55	1.21 s	$^{266}_{105}$	8.19	121.8 min	$^{266}_{104}$	7.50	20.09 h
$^{265}_{109}$	11.07	0.178 ms	$^{265}_{107}$	9.77	74.4 ms	$^{265}_{105}$	8.49	1.76 min	$^{265}_{104}$	7.78	6.58 h
$^{264}_{107}$	9.97	74.1 ms	$^{264}_{106}$	9.21	0.60 s	$^{264}_{105}$	8.66	154 s	$^{264}_{104}$	8.14	5.03 min
$^{263}_{108}$	10.67	1.52 ms	$^{263}_{107}$	10.08	11.6 ms	$^{263}_{105}$	9.01	2.4 s	$^{263}_{104}$	8.49	76.8 s
$^{262}_{107}$	10.30	9.51 ms	$^{262}_{106}$	9.60	47.5 ms	$^{262}_{105}$	9.01	10.9 s	$^{262}_{104}$	8.49	20.6 s
$^{261}_{107}$	10.56	0.74 ms	$^{261}_{106}$	9.80	56.1 ms	$^{261}_{105}$	9.22	0.60 s	$^{260}_{107}$	10.47	3.58 ms
$^{260}_{104}$	8.90	1.08 s	$^{259}_{106}$	9.83	50.5 ms	$^{259}_{105}$	9.62	45.9 ms	$^{259}_{104}$	9.12	0.93 s
$^{258}_{106}$	9.67	36.1 ms	$^{258}_{105}$	9.48	0.42 s	$^{258}_{104}$	9.25	103 ms	$^{257}_{105}$	9.23	0.67 s
$^{257}_{104}$	9.04	1.76 s	$^{256}_{105}$	9.46	522 ms	$^{256}_{104}$	8.93	1.04 s	$^{255}_{105}$	9.72	28.9 ms

[5] G. Royer, *Nucl. Phys. A* **807** (2008) 105.

[6] P. Möller, J.R. Nix, W.D. Myers, W.J. Swiatecki, *At. Data Nucl. Data Tables* **59** (1995) 185.

[7] G. Audi, A.H. Wapstra, C. Thibault, *Nucl. Phys. A* **729** (2003) 337.

[8] G. Royer, B. Remaud, *Nucl. Phys. A* **444** (1985) 477.

[9] G. Royer, *J. Phys. G* **26** (2000) 1149.

[10] J. Blocki, J. Randrup, W.J. Swiatecki, C.F. Tsang, *Ann. of. Phys.* **105** (1977) 427.

[11] I. Angeli, *At. Data Nucl. Data Tables* **87** (2004) 185.

[12] G. Royer, H.F. Zhang, *Phys. Rev. C* **77** (2008) 037602.